Catal Lett (2008) 124:428–433
DOI 10.1007/s10562-008-9496-3

Selective Oxidation of Isobutane and Isobutene to Methacrolein over Te–Mo Mixed Oxide Catalysts

Jingqi Guan · Cheng Xu · Zhuqian Wang · Ying Yang · Bo Liu · Fanpeng Shang · Yanqiu Shao · Qiubin Kan

Received: 5 March 2008 / Accepted: 11 April 2008 / Published online: 30 April 2008

Abstract A series of Te–Mo–O catalysts were prepared by decomposing $(NH_4)_4TeMo_6O_{22} \cdot 2H_2O$ telluromolybdate under different conditions and tested for the oxidation of isobutane and isobutene. Characterization results (XRD, FTIR, TG, TPR, XPS, and BET) showed that their structure and properties depend on calcination conditions. Catalytic tests showed that molybdenum may be the key element for the activation of isobutane, whereas the selective oxidation of isobutene to methacrolein (MAL) might proceed mainly on the surface of the TeMo-containing crystalline phase. Thus, relatively high selectivities and yields of MAL and methacrylic acid (MAA) can be obtained over these specially designed catalysts.

Keywords Isobutane · Isobutene · Te–Mo–O catalysts · Selective oxidation · Methacrolein

1 Introduction

Very recently, Mo–V–Te-based mixed oxides possessing multi-functional properties have been reported as potential candidates for the activation of isobutane [1–6]. It has been proposed that Te^{4+} is the important ion to form M1 (TeM_3O_{10}, M = Mo, V and Nb) and M2 ($Te_2M_{20}O_{57}$) phases [7–11]. Furthermore, it is suggested that the selective oxidation of isobutene (i-$C_4^=$) to methacrolein (MAL) and methacrylic acid (MAA) might mainly proceed on the surface of the TeMo-containing crystalline phase [4]. However, since three or more crystalline phases are present in the complicated multicomponent catalysts synthesized by dry-up method and the structure of these materials has not yet been solved, it is comparatively difficult to discuss a phase effect on the oxidation activity. It is, therefore, strongly hoped that catalysts containing simple phases for selective oxidation of isobutane should be designed.

In the past decades, Te–Mo-containing catalysts have been identified to be high active and selective for catalytic oxidation of hydrocarbons, especially for the oxidation of propene [12–14]. The presence of $Te_2MoO_7/TeMo_5O_{16}$ phases is correlated with its high selectivity to aldehydes. Additionally, it is assumed that Te ions, probably in 4+ oxidation state, play an important role in the oxidation of propene to acrolein [7]. However, there have been only few reports on Te–Mo–O mixed oxides catalysts for the selective oxidation of isobutane and isobutene up to now. As far as we are aware, there are few previous literatures concerning the selective oxidation of isobutene [6, 15]. Therefore, investigating catalytic oxidation of isobutane and isobutene over Te–Mo–O system catalysts has great academic interests as well as commercial interests. In this study, we will discuss the catalytic behavior of a series of Te–Mo–O mixed oxides synthesized from $(NH_4)_4TeMo_6O_{22} \cdot 2H_2O$ for the selective oxidation of isobutane and isobutene.

2 Experimental

2.1 Catalyst Preparation

Preparation of $(NH_4)_4TeMo_6O_{22} \cdot 2H_2O$ telluromolybdate has been described elsewhere [14, 16]. Briefly, a mixture of

J. Guan · C. Xu · Z. Wang · Y. Yang · B. Liu · F. Shang · Y. Shao · Q. Kan (✉)
College of Chemistry, Jilin University, Changchun 130023, People's Republic of China
e-mail: qkan@mail.jlu.edu.cn

Y. Shao
Department of Chemistry, Mudanjiang Normal College, Mudanjiang 157012, People's Republic of China

10.0 g (8.09 mmol) of $(NH_4)_6Mo_7O_{24} \cdot 4H_2O$ and 1.506 g (9.43 mmol) of TeO_2 with Mo:Te ratio of 6:1 was autoclaved along with 21.0 mL of water in a Teflon-lined stainless steel reactor at 175 °C for 4 days and then cooled to room temperature over a period of 36 h. The resulting material precursor was obtained after filtered, washed with distilled water and dried at 60 °C for 24 h. The sample will be denoted as HT, which was calcined under a flow of N_2 (50 mL min^{-1}) or air (50 mL min^{-1}) to obtain the catalyst. The calcination was performed with a heating rate of 2 °C min^{-1}. The final calcination temperature was 500 °C for 2 h or 600 °C for 2 h. The samples will be designed as HT-*X*-*Y*, where *X* indicates the final calcination temperature (500 or 600 °C) and *Y* indicates the gas used during the calcination step (A = Air and N = N_2).

For comparative purpose, MoO_3 was prepared from $(NH_4)_6Mo_7O_{24} \cdot 4H_2O$ by calcination at 500 °C for 20 h in an air stream [17].

2.2 Catalyst Characterization

The specific surface areas of the catalysts were measured based on the adsorption isotherms of N_2 at −196 °C using the BET method (Micromeritics ASAP2010). Powder X-ray diffraction (XRD) patterns were collected using a Shimadzu XRD-6000 scanning at 4° min^{-1} with CuKα radiation (40 kV, 30 mA). The infrared spectra (IR) of various samples were recorded at room temperature using a NICOLET Impact 410 spectrometer. TG and DTA measurements were carried out on a Shimadzu DTA-60 working in an air or N_2 stream. The temperature was raised up to 700 °C at a heating rate of 20 °C min^{-1}. X-ray photoelectron spectra (XPS) were recorded on a VG ESCA LAB MK-II X-ray electron spectrometer using AlKα radiation (1486.6 eV, 10.1 kV). The spectra were referenced with respect to the C 1 s line at 284.7 eV. The measurement error of the spectra was ±0.2 eV. Temperature-programmed reduction profiles (from room temperature to 800 °C) were obtained with a thermal conductivity detector using 5% H_2/Ar mixture with a flow rate of 50 cm^3 min^{-1} and a heating rate of 10 °C min^{-1}.

2.3 Catalytic Tests

The catalytic experiments were carried out in a fixed bed quartz tubular reactor (i.d., 16 mm; length, 400 mm), working at atmospheric pressure [4]. Catalyst samples (0.3–0.5 mm particle size) were introduced into the reactor and diluted with 1 g of silicon carbide (0.5–0.75 mm particle size) in order to keep a constant volume in the catalyst bed. The feed consisted of a mixture of *i*-$C_4H_{10}/O_2/N_2/H_2O$ and *i*-$C_4H_8/O_2/N_2/H_2O$ with a molar ratio of 1/2/2/2 and 1/2/5/2, respectively.

3 Results and Discussion

3.1 XRD Studies

Figure 1 shows the pattern of the as-synthesized sample. Consistent with the observations [14, 16], Te^{4+} ions have been successfully incorporated into the solid forming $(NH_4)_4TeMo_6O_{22} \cdot 2H_2O$. However, the presence of a small amount of TeO_2 in the as-synthesized material cannot be neglected.

Figure 2 provides the XRD patterns of Te–Mo mixed oxide catalysts calcined under different conditions. It can be concluded that $TeMo_5O_{16}$ [JCPDS 88-0407] is a main crystalline phase in samples calcined in N_2, whereas MoO_3 [JCPDS 35-0609] and α-$TeMo_4O_{13}$ [JCPDS 34-0622] are also formed. However, it is evident that MoO_3 and Te_2MoO_7 [30-1339] are main crystalline phases in samples

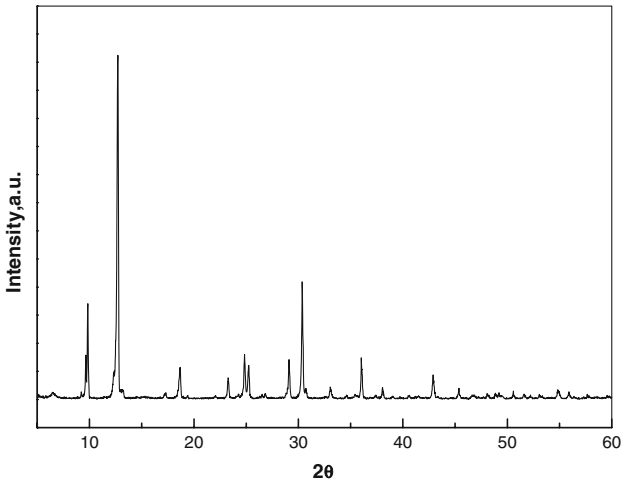

Fig. 1 XRD pattern of as-synthesized sample

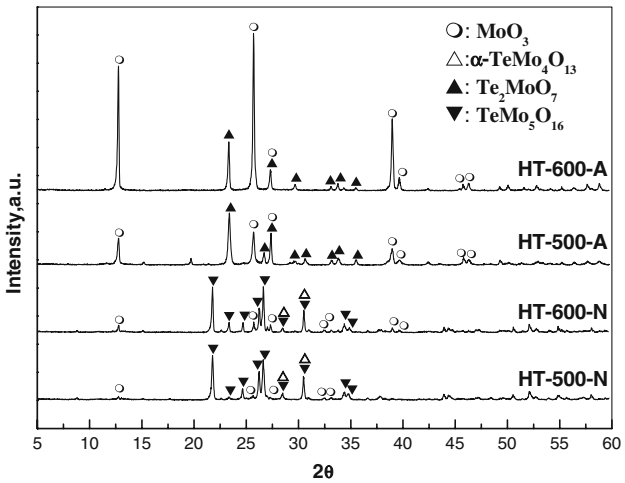

Fig. 2 XRD patterns of Te–Mo mixed oxide catalysts calcined under different conditions

calcined in air. In addition, more MoO_3 is formed during calcination in air, and a Te-rich Mo-oxide phase is formed in consequence, which is contrary to calcination in N_2.

In order to compare the distribution of the crystalline phases in calcined samples, the $TeMo_5O_{16}/MoO_3$ and Te_2MoO_7/MoO_3 ratios have tentatively been determined from the intensities to the more important reflections of each crystalline phase, e.g. [3 0 0] in the $TeMo_5O_{16}$ ($2\theta = 26.6°$), [0 2 2] in the Te_2MoO_7 ($2\theta = 23.4°$), and [0 2 0] in the MoO_3 ($2\theta = 12.7°$). The results of Fig. 2 indicate that the $TeMo_5O_{16}/MoO_3$ ratios are 9.8 for HT-500-N and 6.1 for HT-600-N. In the meanwhile, the Te_2MoO_7/MoO_3 ratios are 1.9 for HT-500-A and 0.4 for HT-600-A. Consequently, the $TeMo_5O_{16}$ (or Te_2MoO_7)/MoO_3 ratios in these samples follow the trend HT-500-N > HT-600-N > HT-500-A > HT-600-A.

3.2 FT-IR Studies

Figure 3 displays the IR spectra of MoO_3 and Te–Mo mixed oxide catalysts calcined under different conditions. It is obvious that the bands at 989, 876, 820, 615, and 514 cm^{-1} are characteristic of MoO_3. However, all of these bands can be shifted from their original positions due to incorporation of Te atoms to the system [8]. For the samples calcined in N_2, the bands at 991, 884, 820, and 505 cm^{-1} can be attributed to MoO_3, whereas the bands at 922, 804, 715, 644, and 586 cm^{-1} should be related to $TeMo_5O_{16}$ phase [4, 8]. Moreover, the bands at 980 and 950 cm^{-1} could be associated to α-$TeMo_4O_{13}$ [14]. However, the FTIR spectra of samples calcined in air are comparatively different from those calcined in N_2. For example, there is only MoO_3 (bands at 991, 864, 820 and 583 cm^{-1}) can be observed for sample HT-600-A. In addition, new bands appear in the IR spectrum of sample HT-500-A. Among them, the band at 771 cm^{-1} is characteristic of α-TeO_2, while the bands at 908 and 644 cm^{-1} can be ascribed to a vitreous TeO_2–MoO_3 [14, 18].

3.3 XPS Studies

To gain deeper insight into the surface constitution and properties of these catalysts, their Mo $3d_{5/2}$ binding energies are investigated and corresponding spectra are composed and integrated with the results shown in Table 1. The Mo $3d_{5/2}$ peak of catalysts could be fitted into two components at 231.7 and 232.8 eV, which can be assigned to Mo^{5+} and Mo^{6+} species, respectively [4, 8, 19]. Thus, the Mo^{6+}/Mo^{5+} surface atomic ratio is found to increase in the sequence HT-600-N < HT-500-N < HT-500-A < HT-600-A. The Te $3d_{5/2}$ peak of catalysts could be fitted into two components at 576.2 and 577.3 eV, which can be related to Te^{4+} and Te^{6+} species, respectively [4]. It is obvious that higher temperature and oxidized ambience favor the formation of Te^{4+}-containing species.

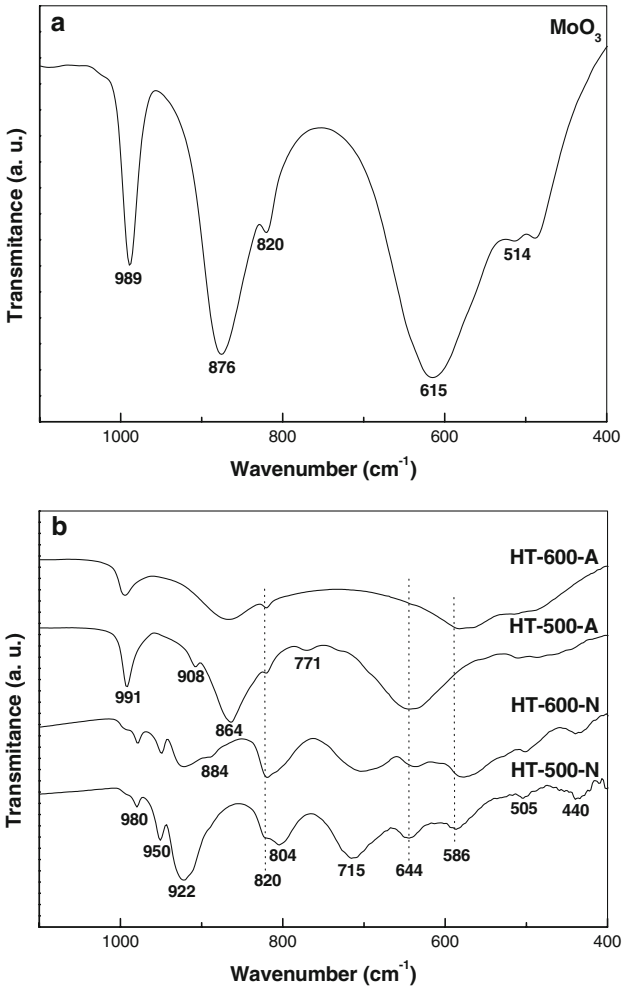

Fig. 3 IR spectra of MoO_3 and Te–Mo mixed oxide catalysts calcined under different conditions

3.4 TG–DTA Analyses

TG–DTA plots of the as-synthesized sample working in N_2 and air streams are presented in Fig. 4. It is clear that the temperatures of endothermic peaks are almost the same for N_2 and air treatments, whereas the total weight loss for N_2 thermal decomposition of $(NH_4)_4TeMo_6O_{22} \cdot 2H_2O$ (13.48%) is more than that for air thermal decomposition of $(NH_4)_4TeMo_6O_{22} \cdot 2H_2O$ (11.92%). The differences in mass loss have two reasons: (1) different decomposition products of NH_4^+/NH_3 and (2) the reducing effect of NH_3 during thermal decomposition in N_2.

3.5 H_2-TPR Studies

H_2-TPR profiles of MoO_3, and Te–Mo mixed oxide catalysts are shown in Fig. 5. There are two peaks of

Table 1 XPS data of samples calcined under different conditions

Sample	Binding energy (eV)			Surface composition (at%)				Surface oxidation states	
	Mo $3d_{5/2}$	Te $3d_{5/2}$	O 1s	Mo	Te	O	Mo/Te	Mo^{6+}/Mo^{5+}	Te^{6+}/Te^{4+}
HT-500-N	232.8	576.6	530.8	25.4	4.4	70.2	5.8	0.75/0.25	0.13/0.87
HT-600-N	232.9	576.3	530.5	21.5	6.3	72.2	3.4	0.56/0.44	0.05/0.95
HT-500-A	233.1	576.7	530.8	24.5	4.6	70.9	5.3	0.90/0.10	0.03/0.97
HT-600-A	233.1	576.7	530.8	23.5	4.5	72.0	5.2	0.94/0.06	0/1

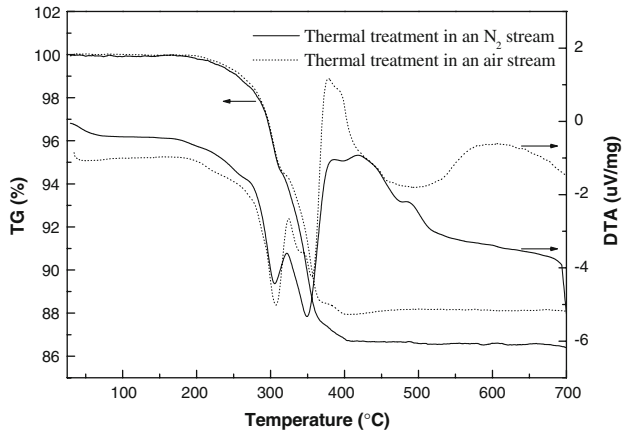

Fig. 4 TG–DTA plots of as-synthesized sample heated in N_2 and air atmosphere

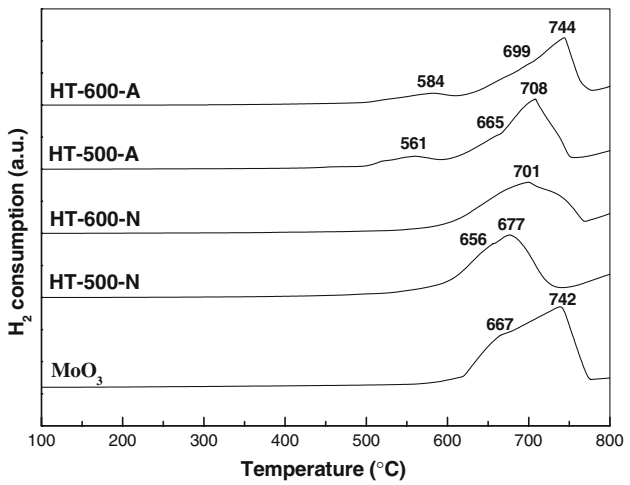

Fig. 5 H_2-TPR profiles of MoO_3 and Te–Mo mixed oxide catalysts calcined under different conditions

H_2-consumption with two maxima at 667 and 742 °C for pure MoO_3, corresponding to the stepwise reduction of $MoO_3 \rightarrow MoO_2$ and $MoO_2 \rightarrow Mo$, respectively [20–22]. The H_2-TPR profile of HT-500-N displays two peaks at 656 and 677 °C, which may be attributed to a stepwise reduction of $MoO_3 \rightarrow Mo_4O_{11}$, and $Mo_4O_{11} \rightarrow MoO_2$, respectively [22, 23]. The reduction behavior of HT-600-N observed in Fig. 5 does not resemble that observed in HT-500-N, in which a broad peak centered at 701 °C is due to the stage of reduction Te^{4+} to Te^0 and a partial reduction of Mo-species [23]. On the other hand, for the sample HT-500-A calcined in air, a first TPR peak appears at about 561 °C, considered to be associated with the reduction of Mo^{6+} to Mo^{4+}, which is distinct from the Mo^{6+}-species reduced at around 667 °C. A similar result was reported by Botto et al. [23] in a study on the reduction behavior of $(NH_4)_3[AlMo_6O_{24}H_6] \cdot 7H_2O$. However, the peak shifts to higher temperature (e.g. 584 °C) if the sample is calcined at 600 °C. These results indicate that the calcined conditions can properly modify the reduction capability of catalysts.

3.6 Catalytic Properties

BET specific surface areas and catalytic behaviors of the five catalysts prepared for this study are listed in Table 2. For a comparative purpose, the catalytic results obtained over MoO_3 are also presented. As it can be seen, all the samples possess very low specific surface areas ($<1.0\ m^2\ g^{-1}$) whatever the calcined conditions change. The effects of calcined conditions on the possible active phases and catalytic behavior of Te–Mo–O catalyst were evaluated, and the results are reported in Table 2. The pure MoO_3 shows relatively high isobutane conversion and isobutene selectivity but relatively low selectivities to MAL and MAA. The conversion of isobutane over the HT-500-N is the lowest, while the maximum conversion can be obtained over the HT-600-A catalyst. The selectivity to MAL and MAA can be considerably improved by the addition of a small amount of Te to the Mo-based system. However, the maximum selectivity to MAL can be achieved over HT-600-N catalyst, whereas the maximum selectivity to MAA has been attained over HT-500-A. Thereby, it seems that molybdenum may be the key element for the activation of isobutane, whereas the selective oxidation of isobutene to MAL might proceed mainly on the surface of the TeMo-containing crystalline phase.

It is of interest that the catalyst calcined in N_2 at 600 °C presents selectivities to isobutene and MAL higher than the

Table 2 Catalytic properties of the catalysts for isobutane oxidation at 380 °C[a]

Catalysts	S_{BET} (m^2 g^{-1})	Conversion (%)	Selectivity (%)							
			i-$C_4^=$	MAL	MAA	CO	CO_2	$C_3^=$	ACT	HAC
MoO_3	0.8	22.2	37.7	14.7	2.1	20.4	6.4	8.5	3.2	6.9
HT-500-N	0.8	19.9	6.4	27.6	7.0	29.7	13.7	6.6	1.0	7.9
HT-600-N	0.3	20.0	21.3	33.5	3.8	18.2	8.1	7.8	2.7	4.5
HT-500-A	0.7	20.1	8.7	26.5	16.7	27.9	10.5	7.4	1.1	1.2
HT-600-A	0.2	26.2	28.9	23.5	6.2	19.9	7.1	7.7	3.3	3.3

[a] Operating condition: GHSV = 3000 mL h^{-1} g_{cat}^{-1}, P = 101 kPa. Symbols: $C_3^=$—propene; ACT—acetone; HAC—acetic acid

corresponding sample calcined in N_2 at 500 °C. Since $TeMo_5O_{16}$ is mainly observed in these catalysts and the $TeMo_5O_{16}/MoO_3$ ratio in HT-500-N is higher than in HT-600-N. It can be suggested that the presence of $TeMo_5O_{16}$ phase in the catalysts favors the transformation of isobutene to MAL, while appropriate MoO_3 can contribute to obtain higher catalyst stability, increasing the selectivity to partial oxidation products during the oxidation of C_3–C_4 olefins [24–26]. On the other hand, it is very similar that the selectivity to isobutene over the catalyst calcined in air at 500 °C is lower than that over the catalyst calcined in air at 600 °C. According to the XRD results, mixed Te_2MoO_7/MoO_3 are the dominant phases in these catalysts, but the Te_2MoO_7/MoO_3 ratio in HT-500-A is higher compared to HT-600-A catalyst. It is therefore rational to suppose that Te_2MoO_7 is also a selective phase in the oxidation of isobutene to MAL. However, it is worthy to mention that a maximum selectivity (16.7%) to MAA has been achieved over HT-500-A. Thus, it is believed that the active sites for the transformation of isobutane to MAA should be a mixture of Te_2MoO_7 and MoO_3 phases.

The reaction results of selective oxidation from isobutene to MAL over the catalysts at 400 °C are summarized in Table 3. It can be seen that the catalytic activity decreases as follows: HT-500-N > HT-600-N > HT-500-A > HT-600-A > MoO_3. As mentioned in the discussion of XRD results, the $TeMo_5O_{16}$(or Te_2MoO_7)/MoO_3 ratios in these samples follow: HT-500-N > HT-600-N > HT-500-A > HT-600-A > MoO_3. Consequently, it has been concluded that $TeMo_5O_{16}$ or Te_2MoO_7 acts as a positive factor in the selective oxidation of isobutene to MAL and is suggested to be active phases in the isobutene oxidation. However, the selectivities to MAL over the Te–Mo–O catalysts vary slightly, which indicates that $TeMo_5O_{16}$ is similarly active and selective as Te_2MoO_7. On the other hand, it may be assumed the Mo^{6+}/Mo^{5+} surface atomic ratio detected by XPS should not be the key factor in the formation of MAL, although Mo^{6+} species are generally accepted to be involved in the selective O insertion of olefinic intermediate [10, 27].

Table 3 Catalytic properties of the catalysts for isobutene oxidation at 400 °C[a]

Catalysts	Conversion (%)	Selectivity (%)						
		MAL	MAA	CO	CO_2	$C_3^=$	ACT	HAC
MoO_3	25.8	38.8	4.3	18.7	27.8	1.2	3.8	5.4
HT-500-N	60.7	64.0	2.9	9.9	14.6	0.4	0.9	7.3
HT-600-N	47.6	63.7	4.9	9.3	14.5	0.7	1.2	5.7
HT-500-A	41.4	62.5	7.4	9.6	14.4	2.2	2.2	1.7
HT-600-A	35.2	68.4	3.5	6.8	13.4	0.9	5.4	1.6

[a] Operating condition: GHSV = 1800 mL h^{-1} g_{cat}^{-1}, P = 101 kPa. Symbols are as in Table 2

In addition, it can be concluded that the selectivity to MAL in the selective oxidation of isobutene over Te–Mo–O catalysts is generally far higher than that in the selective oxidation of isobutane. Therefore, it is reasonable to propose that MAA is formed following a parallel-consecutive scheme: the consecutive path of the reaction may include the steps: isobutene → MAL → MAA → CO_x. The extent of the successive reactions (selectivity to the products rich in oxygen) will increase with the increase in total conversion of isobutane.

4 Conclusions

From the results displayed in this paper, it is apparent that Te–Mo–O catalysts synthesized from $(NH_4)_4TeMo_6O_{22} \cdot 2H_2O$ are active and selective for the oxidation of isobutane and isobutene to MAL, especially, for the latter case. However, the calcination conditions strongly influence the nature of crystalline phases, reducibility, surface composition, and the catalytic performance of these materials in the title reaction. In agreement with our previous studies [4], Mo is the active site for the selective oxidation of isobutane to MAL, whereas isobutene oxidation to MAL occurs over a TeMo-containing phase ($TeMo_5O_{16}$ or Te_2MoO_7). In this way, the $TeMo_5O_{16}$(or Te_2MoO_7)/MoO_3 ratios in the

catalysts have an important effect in MAL selectivity due to synergetic effects between $TeMo_5O_{16}$ (or Te_2MoO_7) and MoO_3.

Acknowledgments We acknowledge the financial supports from the National Basic Research Program of China (2004CB217804) and the National Natural Science Foundation of China (20673046).

References

1. Guan J, Jing S, Wu S, Xu H, Wang Z, Kan Q (2007) React Kinet Catal Lett 90:27
2. Guan J, Jia M, Jing S, Wang Z, Xing L, Xu H, Kan Q (2006) Catal Lett 108:125
3. Guan JQ, Wu SJ, Jia MJ, Huang JH, Jing SB, Xu HY, Wang ZL, Zhu WC, Xing HJ, Wang HS, Kan QB (2007) Catal Commun 8:1219
4. Guan JQ, Wu SJ, Wang HS, Jing SB, Wang GJ, Zhen KJ, Kan QB (2007) J Catal 251:354
5. Andre D, Belletti A, Cavani F, Degrand H, Dubois J-L, Lucarelli C, Trifirò F (2004) DGMK Tagungsbericht 289
6. André D, Belletti A, Cavani F, Degrand H, Dubois J-L, Trifirò F (2005) Stud Surf Sci Catal 155:57
7. Ueda W, Oshihara K, Vitry D, Hisano T, Kayashima Y (2002) Catal Surv Japan 6:33
8. Botella P, López Nieto JM, Solsona B, Mifsud A, Márquez F (2002) J Catal 209:445
9. Aouine M, Dubois JL, Millet JMM (2001) Chem Commun 1180
10. Grasselli RK, Burrington JD, Buttrey DJ, DeSanto P Jr, Lugmair CG, Volpe AF Jr, Weingand T (2003) Top Catal 23:5
11. Millet JMM, Roussel H, Pigamo A, Dubois JL, Jumas JC (2002) Appl Catal A 232:77
12. Bart JCJ, Bossi A, Petrini G, Battiston G, Castellan A, Covini R (1983) Appl Catal 6:85
13. Grzybowska B, Mazurkiewicz A, Stoczyński J (1985) Appl Catal 13:223
14. Botella P, López Nieto JM, Solsona B (2002) J Mol Catal A: Chem 184:335
15. Zhiznevskii VN, Fedevich YV, Sulima IM (1971) Petro Chem USSR 11:157
16. Balraj V, Vidyasagar K (1999) Inorg Chem 38:1394
17. Vande Putte D, Hoonrnaerts S, Thyrion FC, Ruiz P, Delmon B (1996) Catal Today 32:255
18. Dimitriev Y, Bart JCJ, Dimitrov V, Arnaudov M (1981) Z Anorg Allg Chem 479:229
19. Zhu Y, Lu W, Li H, Wan H (2007) J Catal 246:382
20. Parmaliana A, Arena F, Frusteri F (1997) Stud Sturf Sci Catal 110:347
21. Adamski A, Sojka Z, Dyrek K (1999) Langmuir 15:5733
22. Guan JQ, Wang GJ, Jing SB, Wang ZL, Kan QB (2006) Pol J Chem 80:1397
23. Botto IL, Cabello CI, Thomas HJ (1997) Mater Chem Phys 47:37
24. Forzatti P, Trifiró F, Villa PL (1978) J Catal 55:52
25. Weng LT, Ruiz P, Delmon B, Duprez D (1989) J Mol Catal 52:349
26. Yu Adzhmov K, Agaguseinova MM, Khanmamedova AK, Alkhazov TG (1979) Kinet Catal 20:1036
27. Botella P, Concepción P, López Nieto JM, Moreno Y (2005) Catal Today 99:51